Published in final edited form as:
Eur J Neurosci. 2001 April ; 13(7): 1420–1428.

NMDA-evoked calcium transients and currents in the suprachiasmatic nucleus:

gating by the circadian system

Christopher S. Colwell
Mental Retardation Research Center, Department of Psychiatry and Biobehavioural Sciences, University of California, Los Angeles, 760 Westwood Plaza, Los Angeles, CA 90024, USA

Abstract

A variety of evidence suggests that the effects of light on the mammalian circadian system are mediated by glutamatergic mechanisms and that the *N*-methyl-D-aspartate (NMDA) receptor plays an important role in this regulation. One of the fundamental features of circadian oscillators is that their response to environmental stimulation varies depending on the phase of the daily cycle when the stimuli are applied. For example, the same light treatment, which can produce phase shifts of the oscillator when applied during subjective night, has no effect when applied during the subjective day in animals held in constant darkness (DD). We examined the hypothesis that the effects of NMDA on neurons in the suprachiasmatic nucleus (SCN) also vary from day to night. Optical techniques were utilized to estimate NMDA-induced calcium (Ca^{2+}) changes in SCN cells. The resulting data indicate that there was a daily rhythm in the magnitude and duration of NMDA-induced Ca^{2+} transients. The phase of this rhythm was determined by the light—dark cycle to which the rats were exposed with the Ca^{2+} transients peaking during the night. This rhythm continued when animals were held in DD. γ-Aminobutyric acid (GABA)ergic mechanisms modulated the NMDA response but were not responsible for the rhythm. Finally, there was a rhythm in NMDA-evoked currents in SCN neurons that also peaked during the night. This study provides the first evidence for a circadian oscillation in NMDA-evoked Ca^{2+} transients in SCN cells. This rhythm may play an important role in determining the periodic sensitivity of the circadian systems response to light.

Keywords

calcium; circadian rhythms; fura2; NMDA; Rattus rattus; SCN; suprachiasmatic nucleus

Introduction

Most organisms, including humans, exhibit daily rhythms in their behaviour and physiology. In most cases, endogenous processes referred to as circadian oscillators generate these rhythms. These oscillators provide temporal structure to an organism's physiological processes. Nearly all functions of the body show significant daily variations including arousal, metabolism, hormone secretion, learning and memory, motor performance and perception (e.g. Minors & Waterhouse, 1981; Lemmer, 1996; Arendt, 1998). In mammals, the part of the nervous system responsible for most circadian behaviour can be localized to a pair of structures in the hypothalamus known as the suprachiasmatic nucleus (SCN). The circadian oscillator located in these cells generates a rhythm that repeats with a frequency of close to but not equal to 24 h. In order to function adaptively, these cells must be synchronized to the exact 24 h cycle of

Correspondence: Dr C. Colwell, as above. E-mail: ccolwell@mednet.ucla.edu.

the physical world. The daily cycle of light and dark is the dominant cue used by organisms to synchronize their biological clocks to the environment. Thus, a major goal of research in this area is to understand the mechanisms by which light acts to synchronize circadian oscillators.

The SCN receive photic information directly through a monosynaptic projection from the retina known as the retinal hypothalamic tract (RHT) as well as through an indirect connection from the intergeniculate leaflet (Moore, 1996; Ibata *et al*., 1999). The RHT appears to be necessary and sufficient for entrainment by light, and thus a focal point of research in this area has been to identify the transmitters released by the RHT and the resulting signal transduction cascades activated in the SCN. There is now very good evidence that glutamate mediates the effects of light on the circadian system through its role as a transmitter at the RHT—SCN synaptic connection (de Vries *et al*., 1994; Colwell & Menaker, 1996; Ebling, 1996). In the simplest case, light causes the release of glutamate that initiates a signal-transduction cascade in SCN neurons that ultimately results in a phase shift of the circadian system. Based on experience with other signalling systems, calcium (Ca^{2+}) is likely to play a pivotal role in linking glutamate receptor (GluR) activation and other events in the input pathway to the circadian system.

In order to address this hypothesis, this study utilized optical imaging techniques and fura2-AM to measure Ca^{2+} levels in SCN cells in a brain slice preparation. As a first step, a day—night comparison was made between Ca^{2+} transients evoked by *N*-methyl-D-aspartate (NMDA) in SCN slices from animals maintained in a light—dark (LD) cycle. Animals from a reversed LD cycle were used to confirm that the phase of the rhythm was determined by the prior LD cycle. Next, experiments determined whether any diurnal variation would remain when animals were placed in constant darkness (DD), a hallmark feature of a circadian rhythm. Finally, whole-cell patch electrophysiological techniques were used to directly measure NMDA currents in SCN neurons and to determine if the magnitude of these currents varied from day to night.

Materials and methods

Animals and brain slice preparation

The UCLA Animal Research Committee approved the experimental protocols used in this study. Brain slices were prepared using standard techniques from rats (Sprague-Dawley) between 10 and 15 days of age. For reasons that are not completely understood, infrared differential interference contrast (IR DIC) videomicroscopy and dye loading with acetoxymethyl (AM) esters works better in slices from young animals. The circadian oscillator based in the SCN is functional by this age (e.g. Reppert & Schwartz, 1984; Shibata & Moore, 1987). Rats were killed by decapitation, brains dissected and placed in cold oxygenated artificial cerebral spinal fluid (ACSF) containing (in mM): NaCl, 130; $NaHCO_3$, 26; KCl, 3; $MgCl_2$, 5; NaH_2PO_4, 1.25; $CaCl_2$, 1.0; and glucose 10 (pH 7.2–7.4; osmolality 290–300 mosm). After cutting slices, transverse sections (350 μm) were placed in ACSF (25–27 °C) for at least 1 h (in this solution $CaCl_2$ was increased to 2 mM AND $MgCl_2$ was decreased to 2 mM). Slices were constantly oxygenated with 95%O_2-5% CO_2. Slices were placed in a perfusion chamber (Warner Instruments, Hamden, CT, USA) attached to the stage of the fixed-stage upright microscope. The slice was fixed with thin nylon threads glued to a platinum wire and submerged in continuously flowing, oxygenated ACSF at 2 mL/min. Solution exchanges within the slice were achieved by a rapid gravity feed delivery system. In our system, the effects of bath-applied drugs began within 15 s and were typically complete by 1–2min.

IR DIC videomicroscopy

Slices were viewed with an upright compound microscope (Olympus BX50, Melville, NY, USA), using a water immersion lens (40 ×) and DIC optics. They were illuminated with near

IR light by placing an IR bandpass filter (750–1050 nm) in the light path. The image was detected with an IR-sensitive video camera (Hamamatsu C2400, Bridgewater, NJ, USA) and displayed on a video monitor. A camera controller allowed analogue contrast enhancement and gain control. Cells were typically visualized from 30 to 100 μm below the surface of the slice. In the present study, IR videomicroscopy was utilized to visualize cells within the brain slice and to limit some of the uncertainty as to the cell type. This imaging technique allowed us to clearly view the SCN and to exclude cells from the surrounding hypothalamic regions. In addition, morphological criteria were used to target SCN neurons and to avoid taking measurements from cells that were clearly glia. Although size is hardly foolproof, in a few cases, electrophysiological recording and fluorescent imaging were combined to demonstrate that the cells from which Ca^{2+} levels were being measured indeed show the electrical properties of neurons ($n = 5$). Accordingly, it is likely that most of the data were collected from SCN neurons.

Whole-cell patch clamp electrophysiology

Methods were similar to those described previously (Colwell *et al*., 1998). Briefly, electrodes were pulled on a multistage puller (Sutter, P-97, Novato, CA, USA). Electrode resistance in the bath was typically 4–6 MΩ. The standard solution in the patch pipette contains (in mM): Cs-methanesulphonate, 125; EGTA, 9; Hepes, 8; MgATP, 8; NaCl, 4; KCl, 3; and $MgCl_2$, 1. The pH was between 7.25 and 7.3 and the osmolality was between 280 and 290 mosm. Whole-cell recordings were obtained with an Axon Instruments 200B amplifier and monitored online with pCLAMP (Axon Instruments, Foster City, CA, USA). To minimize changes in offset potentials with changing ionic conditions, the ground path used an ACSF agar bridge. Cells were approached with slight positive pressure (2–3 cm H_2O) and offset potentials were corrected. The pipette was lowered to the vicinity of the membrane keeping a positive pressure. After forming a highresistance seal (2–10 GΩ) by applying negative pressure, a second pulse of negative pressure was used to break the membrane. While entering the whole-cell mode, a repetitive test pulse of 10 mV was delivered in a passive potential range (≈ –60 to –70 mV). Whole-cell capacitance and electrode resistance were neutralized and compensated (50–80%) using the test pulse; data acquisition was then initiated. Series and input resistances were monitored throughout the experiment by checking the response to small pulses in a passive potential range. The access resistance of these cells ranged from 20 to 40 MΩ whereas the cell capacitance was typically between 8 and 12 pF.

The current required to maintain the cell's membrane potential at –70 mV was monitored throughout the experiment. In addition, the neuron's current-voltage relationship was measured every 2–3min by moving the cells membrane potential through a ramp of voltages. In these experiments, after the initial control ramps (no drug), each cell was exposed to one concentration of NMDA followed by a wash until the response returned to baseline. The NMDA-evoked currents were determined from neurons using a ramp command voltage from –70 mV to +40 mV (over 5 s) and then back to –90 mV (1 s). All data were collected from the downward ramp. Current—voltage relationships were calculated as the response to the agonist minus the baseline response in the absence of the agonist. This approach has been used successfully to assess voltage-dependent currents in neocortical and neostriatal cells (Burgard & Hablitz, 1994; Cepeda *et al*., 1995).

Calcium imaging

A cooled CCD camera (Microview model 1317 × 1035 pixel format; Princeton Instruments, Monmouth Junction, NJ, USA,) was added to the Olympus fixed stage microscope to measure fluorescence. In order to load the dye into cells, slices were incubated in membrane permeable fura2 AM (50 μM, Molecular Probes) at 37 °C for 10min. The fluorescence of fura2 was excited alternatively at wavelengths of 357 nm and 380 nm by means of a high-speed wavelength-

switching device (Sutter, Lambda DG-4). Image analysis software (MetaFlour, Universal Imaging, West Chester, PA, USA) allowed the selection of several 'regions of interest' within the field from which measurements are taken. In order to minimize bleaching, the intensity of excitation light and sampling frequency was kept as low as possible. In these experiments the intensity of excitation light was measured as 18 μW out of the objective and measurements were normally made once every 2 s.

Calibration of Ca^{2+} signals

Free $[Ca^{2+}]$ was calculated from the ratio (R) of fluorescence at 357 and 380 nm, using the following equation: $[Ca^{2+}] = K_d \times Sf \times (R - R_{min})/(R_{max} - R)$ (Grynkiewicz *et al*., 1985). The K_d was assumed to be 135 nM whereas values for R_{min} and R_{max} were all determined via calibration methods. Initially an *in vitro* method was used to make estimate values. With this method, rectangular glass capillaries were filled with high Ca^{2+} (fura2 + 10 mM Ca^{2+}), low Ca^{2+} (fura2 + 10 mM EGTA) and a control solution without fura2. The fluorescence (F) at 380 nm excitation of the low Ca^{2+} solution was imaged and the exposure of the camera adjusted to maximize the signal. These camera settings were then fixed and measurements were made with 380 and 357 nm excitation of the three solutions. R_{min} = F357nm in low Ca^{2+}/F380 in low Ca^{2+} R_{max} = F357 in high Ca^{2+}/F380 in high Ca^{2+} Sf = F380 in low Ca^{2+}/F380 in high Ca^{2+}. In addition, an *in vivo* calibration method was also used. For this, SCN cells were loaded via the patch pipette using solutions inside the electrode similar to the normal internal solution but containing either no Ca^{2+} (20 mM EGTA) or 10 mM Ca^{2+} for R_{min} and R_{max}, respectively.

Lighting conditions

In order to look for possible diurnal variation in NMDA-induced Ca^{2+} transients, animals were maintained on a daily light-dark cycle consisting of 12 h of light followed by 12 h of dark. It is already well established that cells in the SCN continue to show circadian oscillations when isolated from the animal in a brain slice preparation (e.g. Welsh *et al*., 1995). Accordingly, care must be taken as to the time in the daily cycle when the data are collected. Some of the animals were killed 30 min before the time that the lights would have turned off in the LD cycle. The data from these animals were collected between Zeitgeber time (ZT) 14–18 and pooled to form a 'night' group. For comparison, some of the animals were killed immediately after the lights came on. The data from these animals were collected between ZT 2–6 and pooled to form a 'day' group.

Statistical analyses

Between group differences were evaluated using *t*-tests or Mann—Whitney rank sum tests when appropriate. Values were considered significantly different if $P < 0.05$. All tests were performed using SigmaStat (SPSS, Chicago, IL, USA). In the text, values are shown as mean ± SEM.

Results

Data were collected from a total of 1413 cells from 104 animals. All groups contained data from at least four animals. Each of these cells were determined to be within the SCN by directly visualizing the cell's location with IR DIC videomicroscopy before any Ca^{2+} data was collected. A bulk loading procedure was used to load cells with a membrane permeable form of the Ca^{2+} indicator dye fura2. This procedure loads many cells in SCN slices from young animals (10–15-day-old rats were used in the current study). Cells that exhibited uneven loading due to dye sequestration were not included in the data set. Small cell types including glia were easily identified and were not included in the data set. In five cases, a single cell was filled with the Ca^{2+} indicator dye by loading through a patch pipette. In each case, the cell could generate action potentials and thus had the electrical properties of a neuron.

NMDA-induced Ca^{2+} transients were measured in SCN cells

Bath application of NMDA (1–100 μM, 60–300 s, by day) caused Ca^{2+} transients in SCN cells in the brain slice (Fig. 1, top panel). For example, NMDA (50 μM, 60 s) produced an average increase in Ca^{2+} of 47 ± 6% or increased estimated free $[Ca^{2+}]_i$ from 135 to 195 nM (n = 64). This response was widespread within the SCN with 94% of cells examined showing a Ca^{2+} increase of 5% or greater. The average duration of the response (measured as the amount of time the signal was at least 50% of its peak value) was 84 s with Ca^{2+} levels in most of these cells returning to baseline levels within 120 s. NMDA-induced Ca^{2+} transients were blocked by treatment with the competitive NMDA GluR antagonist, 2-amino-5-phosphonovalerate (AP5; 50 μM + NMDA, 3 ± 1%, n = 32, $P < 0.001$; Fig. 1, bottom panel) but not by the AMPA/kainate GluR antagonist, 6-cyano-7-nitroquinoxaline-2,3-dione (CNQX). In addition, NMDA transients were dramatically enhanced by the removal of magnesium (Mg^{2+}) from the extracellular solution (50 μM NMDA, 127 ± 15%, n = 39; Fig. 2). Finally, because Ca^{2+} influx through voltage-activated channels may be a major source of NMDA-evoked Ca^{2+} increases, experiments were performed in the presence of the sodium (Na^+) channel blocker tetrodotoxin (TTX) and the Ca^{2+} channel blocker methoxyverapamil. The latter blocker has been reported to suppress voltage-gated Ca^{2+} channels without affecting NMDA-mediated responses (e.g. Schneggenburger *et al*., 1993). Electrophysiological techniques were used to confirm that application of TTX (1 μM) blocked voltage-gated Na^+ currents and methoxyverapamil (D600, 100 μM) significantly inhibited (> 90%, n = 5) high-voltage activating Ca^{2+} currents in SCN neurons. In the presence of these channel blockers and the absence of Mg^{2+}, bath application of NMDA (50 μM) still produced significant Ca^{2+} transients (68 ± 6%, n = 83; Fig. 2) so the remaining experiments were all conducted in the presence of both TTX and methoxyverapamil.

Circadian rhythm in the magnitude of NMDA-induced Ca^{2+} transients

The next experiment was designed to determine whether Ca^{2+} transients evoked by bath application of NMDA in SCN neurons varied between day and night. These experiments were performed with brain slices taken from animals during their day and compared to data obtained from brain slices from animals during their night. Rats were killed immediately after lights-on for the ‘day’ group or immediately before lights-off for the ‘night’ group. Other than the time that the animals are killed, all other conditions between the day and night groups remained constant. The data was collected between ZT 2–6 and ZT 14–18 and were pooled to form ‘day’ and ‘night’ groups, respectively.

There was a daily rhythm in Ca^{2+} transients with peak NMDA responses significantly higher (42%) during the night than during the day ($P < 0.001$; Fig. 3, top panel). During the day, bath application of NMDA (50 μM) produced Ca^{2+} transients with an average peak value 68 ± 6% above baseline having increased estimated $[Ca^{2+}]_i$ from 89 ± 2 nM to 150 ± 6 nM (n = 83). The same treatment during the night, caused an average increase of 110 ± 7%, having increased estimated $[Ca^{2+}]_i$ from 83 ± 1 nM to 175 ± 6 nM (n = 102). The NMDA-induced Ca^{2+} transients were also longer during the night with an average duration of 190 s, as opposed to 112 s during the day ($P < 0.001$). By contrast, treatment with a solution high in potassium (K^+, 50 mM, 15 s) produced Ca^{2+} transients that were not different from day to night (day, 101 ± 7 nM increase, n = 83; night, 102 ± 6 nM increase, n = 83).

In order to demonstrate that the phase of the rhythm was determined by the prior LD cycle, a group of animals (n = 8) were housed in a ‘reversed’ LD cycle. Again, peak Ca^{2+} transients were significantly higher ($P < 0.05$) during the night (117 ± 18%, n = 72) then during the day (66 ± 5%, n = 65) suggesting that the observed daily variation is determined by the phase of the LD cycle and not some other unknown variable (Fig. 3, top panel). Finally, in order to demonstrate that any diurnal rhythm is circadian, it is necessary to show that the rhythm continues in DD. For these experiments, animals (n = 8) were placed in DD for 2 days prior

to the preparation of brain slices. The data was collected between circadian time (CT) 2–6 and CT 14–18 and were pooled to form a 'subjective day' and 'subjective night' group. Again, there was a daily rhythm in Ca^{2+} transients with measured values significantly higher during the subjective night ($P < 0.001$; Fig. 3, middle panel). During the subjective night, bath application of NMDA (50 μM) produced Ca^{2+} transients with an average increase of 49 ± 2% or increased estimated $[Ca^{2+}]_i$ from 72 ± 2 nM to 121 ± 3 nM ($n = 89$). During the subjective day, the same treatment raised Ca^{2+} levels 27% with estimated $[Ca^{2+}]_i$ increasing from 76 ± 4 nM to 103 ± 5 nM ($n = 64$). As has been reported previously (Colwell, 2000), in the presence of the ion channel blockers (TTX, D600), there was no significant day—night variation in the resting Ca^{2+} levels (day, 86 ± 2 nM, $n = 210$; night, 79 ± 1 nM, $n = 233$).

GABA receptors could modulate the NMDA response

As most SCN neurons are γ-aminobutyric acid (GABA)ergic and make synaptic connections with other cells within the SCN, the possible role of GABA in the modulation of NMDA-induced responses was examined (Fig. 4). During the day, in the presence of TTX and methoxyverapamil, NMDA-evoked Ca^{2+} transients were reduced by the application of the $GABA_A$ antagonist bicuculline (20 μM bicuculline + NMDA 25 ± 6%, $n = 39$ vs. NMDA 35 ± 4%, $n = 32$, $P < 0.05$). This effect of bicuculline was not seen when experiments were run in the absence of Mg^{2+} in the extracellular solution (bicuculline + NMDA 169 ± 13%, $n = 74$ vs. NMDA 152 ± 13%, $n = 64$). By itself, bath application of GABA (100 μM) produced a modest increase in Ca^{2+} of 14 ± 4% ($n = 197$). This effect of GABA was extremely variable as 44% of the cells sampled showed a Ca^{2+} increase (> 5%) in response to GABA whereas 21% showed a decrease in Ca^{2+}. Although GABAergic mechanisms could modulate the NMDA response in the slice, they are not responsible for the rhythm in the magnitude of NMDA-induced Ca^{2+} transients. In an experiment performed in the presence of bicuculline (20 μM), NMDA (50 μM, 120 s) increased estimated Ca^{2+} levels by 25 ± 6% ($n = 39$) during the day, whereas during the night, the same NMDA treatment increased Ca^{2+} by 70 ± 6% ($n = 46$, $P < 0.01$).

Rhythm in Ca^{2+} transients is also reflected in NMDA-evoked currents in SCN neurons

Whole-cell patch clamp recording techniques were used to directly measure currents evoked by NMDA (25 μM) in SCN neurons. In these experiments, the current required to hold the cell's membrane potential at –70 mV was monitored. In addition, the voltage-dependence of the NMDA-evoked currents was measured by moving the cell through a ramp of voltages (from –70 to 40 then back to –90 mV) before, during, and after treatment with NMDA in the bath. As with the Ca^{2+} imaging experiments, these responses were measured in the presence of TTX and methoxyverapamil. Figure 5, top panel shows an NMDA response recorded using this protocol. Most SCN neurons (75%) exhibited NMDA-evoked currents ($n = 69$). These inward currents were voltage-dependent, i.e. NMDA-evoked currents peaked when the cell was held at a membrane potential between –20 and –40 mV. This voltage-dependence was reduced in Mg^{2+}-free solutions. NMDA-evoked currents were reduced 85% by the addition of the NMDA antagonist AP5 (50 μM; data not shown).

The final experiment was designed to determine whether these inward currents evoked by bath application of NMDA varied between day and night in SCN neurons. As described above, these experiments were performed with brain slices taken from animals during their day and compared to data obtained from brain slices from animals during their night. These experiments were run in the absence of Mg^{2+} to reduce the voltage-dependence of the NMDA response. Because activation of voltage-dependent Na^+, Ca^{2+} and K^+ currents could distort measurement of NMDA-evoked currents, cesium (Cs^+, 125 mM) was used in the patch pipette while tetra-ethylammonium chloride (TEA, 10 mM), cadmium (Cd^{2+}, 25 μM), and TTX (1 μM) were in the bath. Under these conditions, there was a daily rhythm in NMDA-evoked inward currents

with peak responses significantly ($P < 0.05$) higher during the night than during the day (Fig. 5, bottom panel). During the day, NMDA (25 μM, 120–300 s) produced an average peak inward current of –64 ± 7pA ($n = 23$) while, during the night, this same treatment produced an average peak current of –97 ± 13 pA ($n = 21$). This day/night difference was also seen in the magnitude of the change of current needed to hold the neurons at –70 mV during the NMDA treatment (day 180 ± 26%, night 302 ± 35%). NMDA currents were also measured in the presence of Cd^{2+} and TTX (1 μM) but without blockers of K^+ channels. Under these conditions (Fig. 5, bottom panel), it was still possible to measure a daily rhythm with peak currents greater in the night (–105 ± 20pA, $n = 14$) than in the day (–50 ± 14pA, $n = 11$, $P < 0.01$).

Discussion

In the present study, imaging techniques and the indicator dye fura2 were utilized to estimate NMDA-induced Ca^{2+} changes in SCN cells of the mammalian hypothalamus. The resulting data indicate that there was a daily rhythm in the magnitude and duration of NMDA-induced Ca^{2+} transients. The phase of this rhythm was determined by the LD cycle to which the rats were exposed with the Ca^{2+} transients peaking during the night. This rhythm exhibited some of the properties of a circadian oscillation with the rhythm continuing when animals were held in DD. GABAergic mechanisms were found to modulate the NMDA response but were not responsible for the rhythm. Finally, there was a rhythm in NMDA-evoked currents in SCN neurons that also peaked during the night. Overall, the results suggest the presence of a circadian oscillation in NMDA receptor dependent Ca^{2+} transients that may play a role in the regulation of photic information reaching the SCN.

Underlying mechanisms

The Ca^{2+} influx associated with NMDA receptor activation is thought to produce a brief, high-concentration (> 100 μM), localized gradients of Ca^{2+} near open channels (e.g. Neher, 1998; Yuste *et al*., 2000). These gradients are rapidly dissipated by diffusion and binding to buffers and would not be seen by slow, volume-averaged measurements used in the present study. However, these rapid influxes would contribute to the Ca^{2+} load in a slower and diffuse Ca^{2+} pool that is referred to as residual Ca^{2+} (e.g. Tank *et al*., 1995) and it is this pool that we measured with fura2. It may well be that this Ca^{2+} pool in the soma is more directly related to the role of Ca^{2+} as a regulator of gene expression than the faster transients recorded from the dendrites. The free $[Ca^{2+}]_i$ in the cytoplasm results from the highly regulated balance between the rates of Ca^{2+} influx and removal/buffering. Although the present study did not explore the possibility of circadian regulation of Ca^{2+} removal/buffering mechanisms, there is good reason to suspect that the rhythm in NMDA-induced increases in $[Ca^{2+}]_i$ can be accounted for by a daily rhythm in Ca^{2+} influx. Our experimental data indicates that voltage-gated currents certainly contribute to the Ca^{2+} transients (see Fig. 2). In zero Mg^{2+}, NMDA application increased Ca^{2+} levels by 128% while, in the presence of Na^+ and Ca^{2+} channel blockers, the same treatment increased Ca^{2+} by 68%. This suggests that the voltage-sensitive currents are responsible for approximately 50% of the Ca^{2+} transient. Nevertheless, when these currents were blocked, the circadian rhythm in NMDA-evoked Ca^{2+} transients was still present.

The simplest mechanistic explanation for the rhythm in Ca^{2+} transients in the SCN is that the rhythm is a direct result of a daily variation in the magnitude of the NMDA-evoked current. Although the mechanisms underlying this variation in NMDA currents is not known, one possible explanation for these changes in the properties of NMDA receptors is circadian clock regulated changes in the composition of the subunits that comprise NMDA receptors. At least one study has reported day—night differences in the expression of NMDA subunits within the SCN (Ishida *et al*., 1994). Therefore, if the rate of receptor turnover in the SCN membrane is sufficiently rapid, then a daily rhythm in the subunit composition of the NMDA receptor could

be responsible for the observed results. We did not observe any obvious daily change in the voltage-dependence of the NMDA response but did not look at possible daily changes in NMDA receptor kinetics. Alternatively, the NMDA receptors is known to be subject to a wide range of regulatory/modulatory influences including second messenger cascades (e.g. Dingledine *et al*., 1999). Rhythms have now been suggested in a growing number of second messengers systems including calcium (Colwell, 2000), phosphokinase (PK)A (Prosser & Gillette, 1991; Yamazaki *et al*., 1994), and perhaps even PKC (Cagampang *et al*., 1998). Thus it seems likely that the phosphorylation-state of the NMDA receptor may vary from day to night and that this change may underlie the observed rhythm.

NMDA responses are widespread within the SCN

Many of the cells in the SCN express neuropeptides, and differences in peptide expression can serve as a basis to segregate SCN cells. In particular, a distinction is commonly made between cells immunoreactive for vasopressin which are expressed in the rostral and dorsomedial regions and those expressing vasoactive intestinal peptide (VIP +) that are found in the ventrolateral region of the SCN (Card *et al*., 1981; van den Pol & Tsujimoto, 1985). At least one study in rats has directly demonstrated the termination of retinal afferents on VIP+ cells (Tanaka *et al*., 1993). These VIP+ core cells in the SCN must be where the integration of the majority of synaptic inputs are taking place and where we expected to see the most robust NMDA response. However, contrary to our expectations, most cells in the SCN show an excitatory response to NMDA. The application of NMDA caused an increase in firing in 60% of cells monitored extracellularly (Schmahl & Bohwer, 1997), and evoked an inward current in 85% of cells monitored with whole-cell patch recording (Alberi *et al*., 1997). Previous studies have also shown that stimulation of the optic chiasm evokes an excitatory postsynaptic current in most SCN neurons that is mediated in part by NMDA receptors (Kim & Dudek, 1991; Jiang *et al*., 1997). Similarly, we found that up to 94% of Fura2-loaded cells showed a Ca^{2+} increase in response to bath application of NMDA. In our electrophysiological measurements 75% of cells sampled exhibited an NMDA-induced inward current. Although we did not characterize peptide expression in these cells, we did take advantage of video microscopy to visually place neurons within general regions of the SCN. Out of 69 cells from which we recorded NMDA currents, 30 cells were visually judged to be in the dorsomedial and 32 in the ventrolateral regions. There were no significant differences between the currents recorded from one region or the other and certainly, SCN neurons in both the ventrolateral and dorsomedial subdivisions respond to NMDA. This physiological data indicating that most cells within the SCN are capable of being excited by NMDA is consistent with anatomical data suggesting that NMDA receptors are widely distributed within this nucleus (e.g. Mikkelsen *et al*., 1993; Hartgraves & Fuchs, 1994; Stamp *et al*., 1997).

GABA might play a role in modulating responses to NMDA

A variety of evidence suggests that GABA is the major transmitter used by SCN neurons and most SCN neurons send projections to other cells in the SCN (e.g. van den Pol, 1991). Because SCN neurons also exhibit a daily rhythm in neural activity, these cells are likely to be receiving rhythmic GABA-mediated synaptic input. This synaptic input could play a role in modulating the observed rhythm in NMDA-evoked Ca^{2+} transients. In the developing nervous system, including the hypothalamus, it is well established that GABA has the ability to excite cells and increase Ca^{2+} (e.g. Chen *et al*., 1996; Obrietan & van den Pol, 1997). An earlier study (Wagner *et al*., 1997) also reported that in mature SCN neurons, application of GABA can excite cells through a $GABA_A$-dependent mechanism. Interestingly, the effect of GABA on these cells also appears to vary with the time of day as the excitatory response was seen only during the day. While this finding has proven difficult to repeat (Gribkoff *et al*., 1999), it certainly raises the possibility that depolarizing GABA responses could contribute to the NMDA-induced Ca^{2+} transients. Indeed, we found evidence that GABAergic mechanisms can modulate the

NMDA response in the SCN. Specifically, blocking $GABA_A$ receptors actually reduced NMDA-induced Ca^{2+} transients, suggesting that GABA contributes to the excitatory effects of NMDA. In addition, GABA by itself increased Ca^{2+} levels in about 40% of the SCN cells sampled (n = 197). These two observations suggest that, at least in the younger animals used in the current study (postnatal day 10–14), GABA can have 'excitatory' effects on Ca^{2+} levels within SCN neurons. However, because the day—night variation was still seen in the presence of a $GABA_A$ receptor antagonist, GABAergic mechanisms can not be responsible for the rhythm in the magnitude of NMDA-induced Ca^{2+} transients.

Functional importance

One of the fundamental features of circadian oscillators is that their response to environmental stimulation varies depending on the phase of the daily cycle when the stimuli are applied. For example, the same light treatment, which can produce phase shifts of the oscillator when applied during the subjective night, has no effect when applied during the subjective day. This periodic sensitivity to photic stimulation is a central feature of entrainment, i.e. the process by which circadian oscillators are synchronized to the environment. Despite its importance, the cellular and molecular mechanisms behind this differential sensitivity have not been explored in mammals. There is some evidence that this regulation could occur at the level of SCN neurons. Two previous studies have demonstrated a daily rhythm in the response of SCN cells to photic and electrical stimulation of the RHT (Cui & Dyball, 1996; Meijer *et al*., 1996, 1998). In addition, electrical stimulation of the RHT causes the same daily pattern of light-like phase shifts of the circadian system both *in vivo* (de Vries *et al*. 1994) and *in vitro* (Shibata & Moore, 1993), i.e. phase shifts during night but not during day. Finally, exogenous application of GluR agonists cause light-like phase shifts of the circadian rhythm in neuronal activity in the SCN *in vitro* (Ding *et al*., 1994; Shibata *et al*., 1994; Shirakawa & Moore, 1994). The current study adds to this evidence by directly demonstrating that there are daily rhythms in both NMDA-induced Ca^{2+} transients and NMDA currents recorded from SCN neurons in a brain slice preparation. These observations demonstrate that even the most basic property of cell-cell communication in the nervous system, i.e. the response of a cell to postsynaptic stimulation of a receptor, can also vary with the circadian cycle. This raises the possibility that other fundamental properties of cellular communication vary with a daily rhythm.

What are the cellular mechanisms that underlie this periodic sensitivity to environmental stimulation? Work done on the circadian oscillators in the eye of the marine molluscs *Aplysia* and *Bulla* have led to the development of a credible model to explain this daily variation in response to photic stimulation. In these species, specialized retinal cells known as basal retinal neurons or secondary cells show a daily rhythm in membrane potential and spontaneous neural activity (Block *et al*., 1993). Central to the model is the hypothesis that this circadian rhythm in membrane potential drives a rhythm in Ca^{2+} influx through voltage-sensitive Ca^{2+} channels and that light acts to cause a Ca^{2+} influx in these cells (McMahon & Block, 1987; Colwell *et al*., 1992, 1994). During the day, the membrane potential (Vm) is relatively depolarized and Ca^{2+} enters the cell though voltage-sensitive Ca^{2+} channels. Light does not cause phase shifts because $[Ca^{2+}]_i$ is already elevated. During the night, the membrane is relatively hyperpolarized and light-induced depolarization can cause a Ca^{2+} influx leading to a shift in the phase of the rhythm.

We believe that the essence of this molluscan model may be usefully applied to the SCN. Thus our working model for how light synchronizes the mammalian circadian system contains several components. First, RHT fibers are glutamatergic and release glutamate in response to photic stimulation (Colwell & Menaker, 1996; Ebling, 1996). Next, cells in the SCN undergo a daily rhythm in spontaneous electrical activity such that the cells are relatively depolarized and electrically active during the day (e.g. Welsh *et al*., 1995; Jiang *et al*., 1997; de Jeu *et al*.,

1998; Schaap *et al*., 1999). This daily rhythm in spontaneous electrical activity and Vm will have two important consequences for the cells in the SCN. First, these cells will exhibit a daily rhythm in basal Ca^{2+} with resting levels higher during day then during the night. In a recent study, we utilized Ca^{2+} imaging techniques to confirm this prediction of the model and estimated that resting levels during the day averaged 150 nM whereas levels during the night fell to 75 nM (Colwell, 2000). This rhythm appears to be the direct result of high levels of spontaneous electrical activity and resulting Ca^{2+} influx through voltage-dependent channels during the day. Second, the SCN cells will exhibit a daily rhythm in the magnitude of their response to stimulation of the RHT such that responses will be greater during the night than during the day (e.g. Cui & Dyball, 1996; Meijer *et al*., 1996; Meijer *et al*., 1998). The synaptic release of glutamate will always move cells toward the glutamate equilibrium potential. However, in this model, the cell's resting Vm varies as function of time of day. The change in Vm will be greater at night when cells are relatively hyperpolarized compared to day. In addition, in the present study, we have been able to document a rhythm in NMDA-induced Ca^{2+} transients that is most probably driven by a rhythm in NMDA currents. This rhythm could play an important role in determining the periodic sensitivity of the circadian systems response to light.

Acknowledgements

Supported by Whitehall Foundation grant F98P15, NIH HL64582 and MH59186.

Abbreviations

ACSF, artificial cerebral spinal fluid
AP5, 2-amino-5-phosphonovalerate
Ca^{2+}, calcium
Cs^{+}, cesium
CT, circadian time
CNQX, 6-cyano-7-nitroquinoxaline-2,3-dione
DD, dark—dark
DIC, differential interference contrast
GABA, γ-aminobutyric acid
GluR, glutamate receptor
IR, infrared
LD, light—dark
Mg^{2+}, magnesium
NMDA, *N*-methyl-D-aspartate
K^{+}, potassium
RHT, retinohypothalamic tract
Na^{+}, sodium
SCN, suprachiasmatic nucleus
TEA, tetra-ethylammonium chloride
TTX, tetrodotoxin
ZT, Zeitgeber time.

References

Alberi S, Dauphin MD, Dreifuss JJ, Raggenbass M. Whole-cell NMDA-evoked current in suprachiasmatic neurones of the rat: modulation by extracellular calcium ions. Brain Res 1997;745:55–66. [PubMed: 9037394]

Arendt J. Biological rhythms: the science of chronobiology. J. Royal College Physicians London 1998;32:27–35.

Block GD, Khalsa SB, McMahon DG, Michel S, Guesz M. Biological clocks in the retina: cellular mechanisms of biological timekeeping. Int. Rev. Cytology 1993;146:83–144.

Burgard EC, Hablitz JJ. Developmental changes in the voltage-dependence of neocortical NMDA responses. Dev. Brain Res 1994;80:275–278. [PubMed: 7955353]

Cagampang FR, Rattray M, Campbell IC, Powell JF, Coen CW. Variation in the expression of the mRNA for protein kinase C isoforms in the rat suprachiasmatic nuclei, caudate putamen and cerebral cortex. Mol. Brain Res 1998;53:277–284. [PubMed: 9473694]

Card JP, Brecha N, Karten HJ, Moore RY. Immunocytochemical localization of vasoactive intestinal peptide-containing cells and processes in the suprachiasmatic nucleus of the rat. J. Neurosci 1981;1:1289–1303. [PubMed: 7031198]

Cepeda C, Chandler SH, Shumate LW, Levine MS. A persistent Na^+ conductance in medium-size neostriatal neurons: characterization using infrared videomicroscopy and whole-cell patch clamp recordings. J. Neurophysiol 1995;74:1343–1348. [PubMed: 7500155]

Chen G, Trombley PQ, van den Pol AN. Excitatory actions of GABA in developing rat hypothalamic neurones. J. Physiol. (Lond.) 1996;494:451–464. [PubMed: 8842004]

Colwell CS. Circadian modulation of calcium levels in cells in the suprachiasmatic nucleus. Eur. J. Neurosci 2000;12:571–576. [PubMed: 10712636]

Colwell CS, Cepeda C, Crawford C, Levine MS. Postnatal development of NMDA evoked responses in the neostriatum. J. Dev. Neurobiol 1998;20:154–163.

Colwell CS, Khalsa SBS, Block GD. Cellular mechanisms of entrainment. Chronobiol. Intern 1992;9:163–179.

Colwell, CS.; Menaker, M. Regulation of circadian rhythms by excitatory amino acids. In: Brann, DW.; Mahesh, VB., editors. Excitatory Amino Acids: Their Role in Neuroendocrine Function. CRC Press; New York: 1996. p. 223-252.

Colwell CS, Whitmore D, Michel S, Block GD. Calcium plays a central role in phase shifting the ocular circadian pacemaker of Aplysia. J. Comp. Physiol 1994;175:415–423. [PubMed: 7965916]

Cui LN, Dyball REJ. Synaptic input from the retina to the suprachiasmatic nucleus changes with the light-dark cycle in the Syrian hamster. J. Physiol. (Lond.) 1996;497:485–493.

Ding JM, Chen D, Iber ET, Faiman LE, Rea MA, Gillette MU. Resetting the biological clock: mediation of nocturnal circadian shifts by glutamate and no. Science 1994;266:1713–1717. [PubMed: 7527589]

Dingledine R, Borges K, Bowie D, Traynelis SF. The glutamate receptor ion channels. Pharmacol. Rev 1999;51:7–61. [PubMed: 10049997]

Ebling FJP. The role of glutamate in the photic regulation of the suprachiasmatic nucleus. Prog. Neurobiol 1996;50:109–132. [PubMed: 8971980]

Gribkoff VK, Pieschl RL, Wisialowski TA, Park WK, Strecker GJ, de Jeu MT, Pennartz CM, Dudek FE. A reexamination of the role of GABA in the mammalian suprachiasmatic nucleus. J. Biol. Rhythms 1999;14:126–130. [PubMed: 10194649]

Grynkiewicz G, Poenie M, Tsien RY. A new generation of Ca^{2+} indicators with greatly improved fluorescence properties. J. Biol. Chem 1985;260:3440–3450. [PubMed: 3838314]

Hartgraves MD, Fuchs JL. NMDA receptor binding in the rodent suprachiasmatic nucleus. Brain Res 1994;640:113–115. [PubMed: 8004439]

Ibata Y, Okamura H, Tanaka M, Tamada Y, Hayashi S, Iijima N, Matsuda T, Munekawa K, Takamatsu T, Hisa Y, Shigeyoshi Y, Amaya F. Functional morphology of the suprachiasmatic nucleus. Frontiers Neuroendocrinol 1999;20:241–268.

Ishida N, Matsui M, Mitsui Y, Mishina M. Circadian expression of NMDA receptor mRNAs in the suprachiasmatic nucleus of the rat brain. Neurosci. Lett 1994;166:211–214. [PubMed: 8177501]

de Jeu M, Hermes M, Pennartz C. Circadian modulation of membrane properties in slices of rat suprachiasmatic nucleus. Neuroreport 1998;9:3725–3729. [PubMed: 9858386]

Jiang ZG, Yang Y, Liu ZP, Allen CN. Membrane properties and synaptic inputs of suprachiasmatic nucleus neurons in rat brain slices. J. Physiol. (Lond.) 1997;499:141–159. [PubMed: 9061646]

Kim YI, Dudek FE. Intracellular electrophysiological study of suprachiasmatic nucleus neurons in rodents: excitatory synaptic mechanisms. J. Physiol. (Lond) 1991;444:269–287. [PubMed: 1688029]

Lemmer B. The clinical relevance of chronopharmacology in therapeutics. Pharmacol. Res 1996;33:107–115. [PubMed: 8870025]

McMahon DG, Block GD. The Bulla ocular circadian pacemaker. J. Comp. Physiol 1987;161:335–346. [PubMed: 3668876]

Meijer JH, Watanabe K, Detari L, Schaap J. Circadian rhythm in light response in suprachiasmtic nucleus neurons of freely moving rats. Brain Res 1996;741:352–355. [PubMed: 9001742]

Meijer JH, Watanabe K, Schaap J, Albus H, Détári L. Light responsiveness of the suprachiasmatic nucleus: long-term multiunit and single-unit recordings in freely moving rats. J. Neurosci 1998;18:9078–9087. [PubMed: 9787011]

Mikkelsen JD, Larsen PJ, Ebling FJP. Distribution of *N*-methyl-D-aspartate (NMDA) receptor mRNAs in the rat suprachiasmatic nucleus. Brain Res 1993;632:329–332. [PubMed: 8149240]

Minors, DS.; Waterhouse, JM. Circadian Rhythms and the Human. Wright; London: 1981.

Moore RY. Entrainment pathways and the functional organization of circadian. Prog. Brain Res 1996;111:103–119. [PubMed: 8990910]

Neher D. Vesicle pools and Ca^{2+} microdomains: new tools for understanding their roles in neurotransmitter release. Neuron 1998;20:389–399. [PubMed: 9539117]

Obrietan K, van den Pol AN. GABA activity mediating cytosolic Ca^{2+} rises in developing neurons is modulated by cAMP-dependent signal transduction. J. Neurosci 1997;17:4785–4799. [PubMed: 9169537]

van den Pol, AN. The suprachiasmatic nucleus: morphological and cytochemical substrates for cellular interaction. In: Klein, DC.; Moore, RY.; Reppert, SM., editors. Suprachiasmatic Nucleus: the Mind's Clock. Oxford University Press; Oxford: 1991. p. 17-50.

van den Pol AN, Tsujimoto KL. Neurotransmitters of the hypothalamic suprachiasmatic nucleus: immunocytochemical analysis of 25 neuronal antigens. Neuroscience 1985;15:1049–1086. [PubMed: 2413388]

Prosser RA, Gillette MU. Cyclic changes in cAMP concentration and phsophodiesterase activity in a mammalian circadian clock studied in vitro. Brain Res 1991;568:185–192. [PubMed: 1667616]

Reppert SM, Schwartz WJ. The suprachiasmatic nuclei of the fetal rat: Characterization of a functional circadian clock using 2-deoxyglucose. J. Neurosci 1984;4:1677–1682. [PubMed: 6737036]

Schaap J, Bos NP, de Jeu MT, Geurtsen AM, Meijer JH, Pennartz CM. Neurons of the rat suprachiasmatic nucleus show a circadian rhythm in membrane properties that is lost during prolonged whole-cell recording. Brain Res 1999;815:154–166. [PubMed: 9974136]

Schmahl C, Bohwer G. Effects of excitatory amino acids and neuropeptide Y on the discharge activity of suprachiasmatic neurons in rat brain slices. Brain Res 1997;746:151–163. [PubMed: 9037494]

Schneggenburger R, Zhou Z, Konnerth A, Neher E. Fractional contribution of calcium to the cation current through glutamate receptor channels. Neuron 1993;11:133–143. [PubMed: 7687849]

Shibata S, Moore RY. Development of neural activity in the rat suprachiasmatic nucleus. Brain Res 1987;431:311–315. [PubMed: 3040191]

Shibata S, Moore RY. Neuropeptide Y and optic chiasm stimulation affect suprachiasmatic nucleus circadian function in vitro. Brain Res 1993;615:95–100. [PubMed: 8364730]

Shibata S, Watanabe A, Hamada T, Ono M, Watanabe S. *N*-methyl-D-aspartate induces phase shifts in circadian rhythm of neuronal activity of rat SCN in vitro. Am. J. Physiol 1994;267:R360–R364. [PubMed: 7520671]

Shirakawa T, Moore RY. Glutamate shifts the phase of the circadian neuronal firing rhythm in the rat suprachiasmatic nucleus in vitro. Neurosci. Lett 1994;178:47–50. [PubMed: 7816337]

Stamp JA, Piggins HD, Rusak B, Semba K. Distribution of ionotropic glutamate receptor subunit immunoreactivity in the suprachiasmatic nucleus and intergeniculate leaflet of the hamster. Brain Res 1997;756:215–224. [PubMed: 9187335]

Tanaka M, Ichitani Y, Okamura H, Tanaka Y, Ibata Y. The direct retinal projection to VIP neuronal elewents in the rat SCN. Brain Res. Bull 1993;31:637–640. [PubMed: 8518955]

Tank DW, Regehr WG, Delaney KR. A quantitative analysis of presynaptic calcium dynamics that contribute to short-term enhancement. J. Neurosci 1995;15:7940–7952. [PubMed: 8613732]

de Vries MJ, Treep JA, de Pauw ESD, Weijer JH. The effects of electrical stimulation of the optic nerves and anterior optic chiasm on the circadian activity rhythm of the Syrian hamster: involvement of excitatory amino acids. Brain Res 1994;642:206–212. [PubMed: 8032882]

Wagner S, Castel M, Gainer H, Yarom Y. GABA in the mammalian suprachiasmatic nucleus and its role in diurnal rhythmicity. Nature 1997;387:598–603. [PubMed: 9177347]

Welsh DK, Logothetis DE, Weister M, Reppert SM. Individual neurons dissociated from rat suprachiasmatic nucleus express independently phase circadian firing patterns. Neuron 1995;14:697–706. [PubMed: 7718233]

Yamazaki S, Maruyama M, Cagampang FRA, Inouye SIT. Circadian fluctuation of cAMP in the suprachiasmatic nucleus and anterior hypothalamus of the rat. Brain Res 1994;651:329–331. [PubMed: 7922582]

Yuste R, Majewska A, Holthoff K. From form to function: calcium compartmentalization in dendritic spines. Nature Neurosci 2000;3:653–659. [PubMed: 10862697]

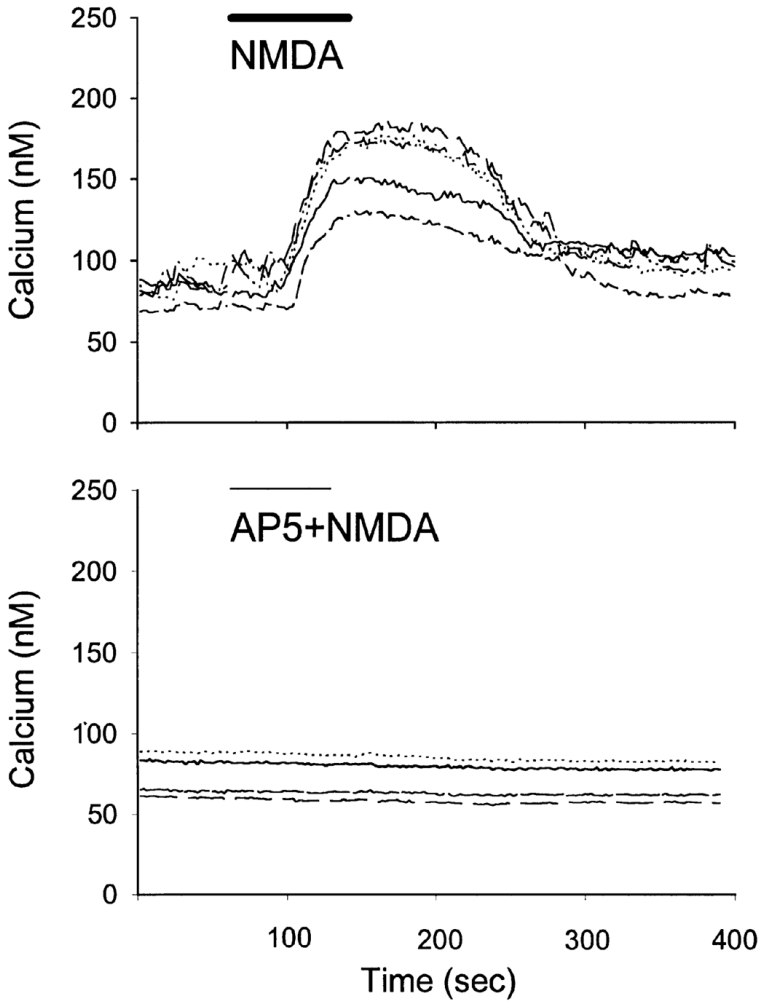

FIG. 1.

Examples of Ca^{2+} transients measured from SCN cells in a brain slice loaded with the Ca^{2+} indicator dye fura2. Each line represents data collected from an individual cell. All of this data was collected in the absence of Mg^{2+} but in the presence of TTX and methoxyverapamil that were included to block voltage-sensitive Na^{+} and Ca^{2+} currents. Top: SCN cells show an increase in Ca^{2+} in response to bath application of NMDA (50 μM, 40 s). Bottom: NMDA-induced Ca^{2+} transients were inhibited by the presence of the NMDA receptor antagonist AP5 (50 μM). Data collected during the night from single SCN slice from a 14-day-old rat.

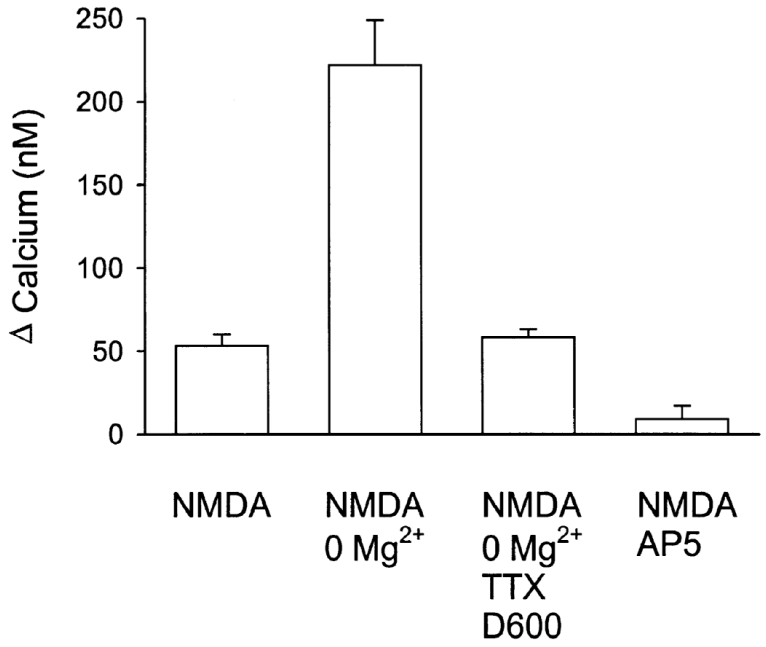

FIG. 2.

NMDA regulation of Ca^{2+} levels in the SCN. Bath application of NMDA (50 μM, 60 s) produced Ca^{2+} transients in most cells (94%) within the SCN ($P < 0.001$, $n = 64$). These NMDA-induced Ca^{2+} transients were blocked by treatment with the NMDA GluR antagonist AP5 (50 μM, $P < 0.001$, $n = 32$) and were enhanced by the removal of magnesium (Mg^{2+}) from the extracellular solution ($P < 0.001$, $n = 39$). Finally, because Ca^{2+} influx through voltage-activated channels might be a major source of NMDA-evoked Ca^{2+} increases, some experiments were run in the presence of the TTX and methoxyverapamil (D600). In the presence of these channel blockers and the absence of Mg^{2+}, bath application of NMDA (50 μM) still produced significant Ca^{2+} transients ($P < 0.001$, $n = 83$). Data collected during day from 10–15-day-old rats.

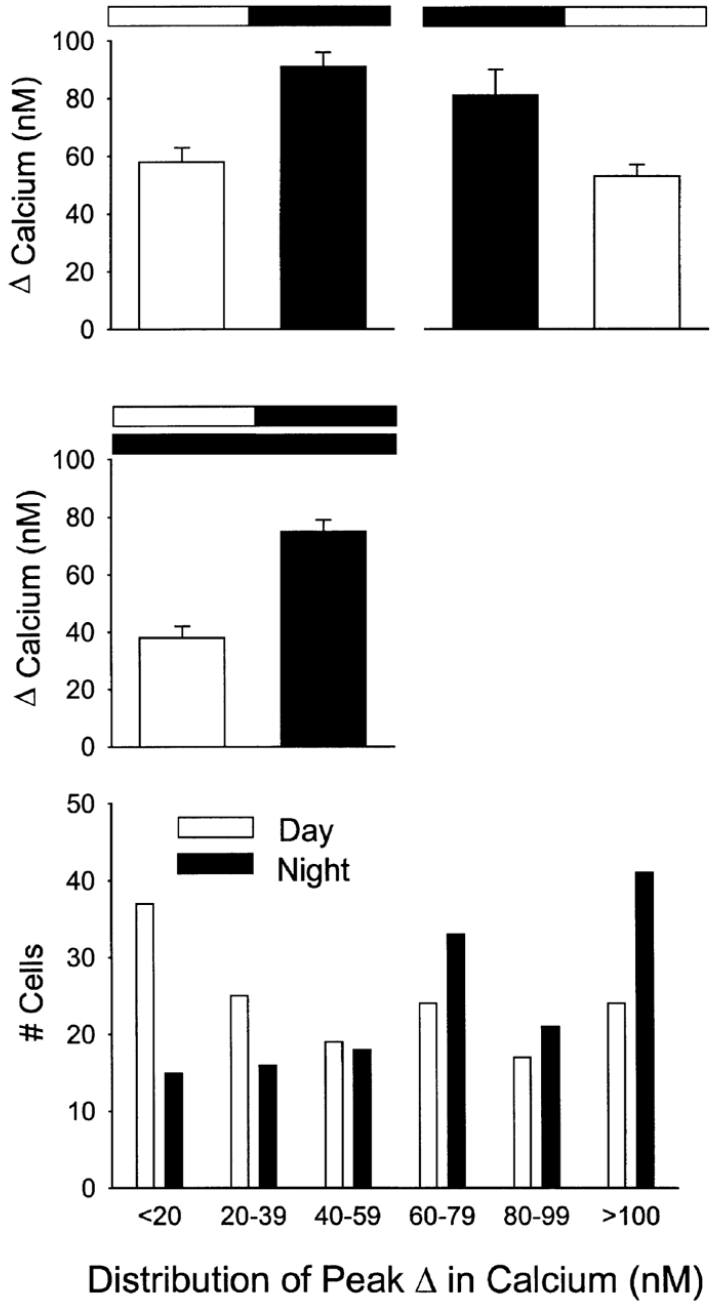

FIG. 3.

Diurnal rhythm in NMDA-evoked Ca^{2+} transients in SCN cells. In these experiments, NMDA-evoked Ca^{2+} transients were measured in SCN neurons in brain slices from animals during their day and compared to data obtained from brain slices from animals during their night. Animals were killed at either ZT 0 for the day group or ZT 12 for the night group. Each cell was sampled only once. Top left panel: NMDA-evoked Ca^{2+} transients peaked during night (day $n = 83$, night $n = 102$, $P < 0.001$). Top right panel: when the phase of the light-dark cycle to which the animals were exposed was reversed, so did the resulting rhythm (day $n = 72$; night $n = 65$, $P < 0.05$). Middle panel: in these experiments, animals were maintained in constant conditions and NMDA-evoked Ca^{2+} transients were measured in SCN neurons in brain slices

from animals during their subjective day and compared to data obtained from brain slices from animals during their subjective night. Once again, NMDA-evoked Ca^{2+} transients peaked during subjective night (day $n = 64$; night $n = 89$, $P < 0.001$). Bottom panel: histogram illustrates the daily variation in the distribution of the NMDA-induced Ca^{2+}responses. As has been previously reported (Colwell, 2000), in the presence of the ion channel blockers (TTX, D600), there was no significant day/night variation in the resting Ca^{2+} levels (day 89 ± 2 nM, $n = 83$; night 83 ± 1 nM, $n = 102$).

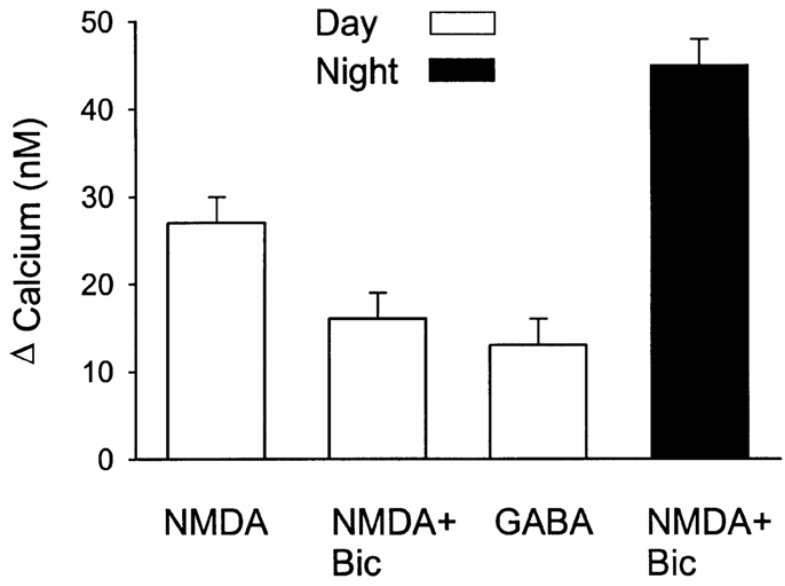

FIG. 4.

GABAnergic modulation of NMDA-evoked Ca^{2+} transients in cells in the SCN. During the day, in the presence of TTX and methoxyverapamil, NMDA-evoked Ca^{2+} transients were reduced by the application of the $GABA_A$ antagonist bicuculline (bicuculline + NMDA n = 39; NMDA $n = 32$, $P < 0.05$). This effect of bicuculline (20 μM) was not seen when experiments were run in the absence of extracellular Mg^{2+}. By itself, bath application of GABA (100 μM) produced a modest increase in Ca^{2+} ($n = 197$). This effect of GABA was extremely variable as 44% of the cells sampled showed a Ca^{2+} increase (> 5%) in response to GABA whereas 21% showed a decrease in Ca^{2+}. In an experiment run in the presence of bicuculline, it was still possible to see a day—night difference in the magnitude of NMDA-induced Ca^{2+} transients (day $n = 39$; night $n = 46$; $P < 0.01$).

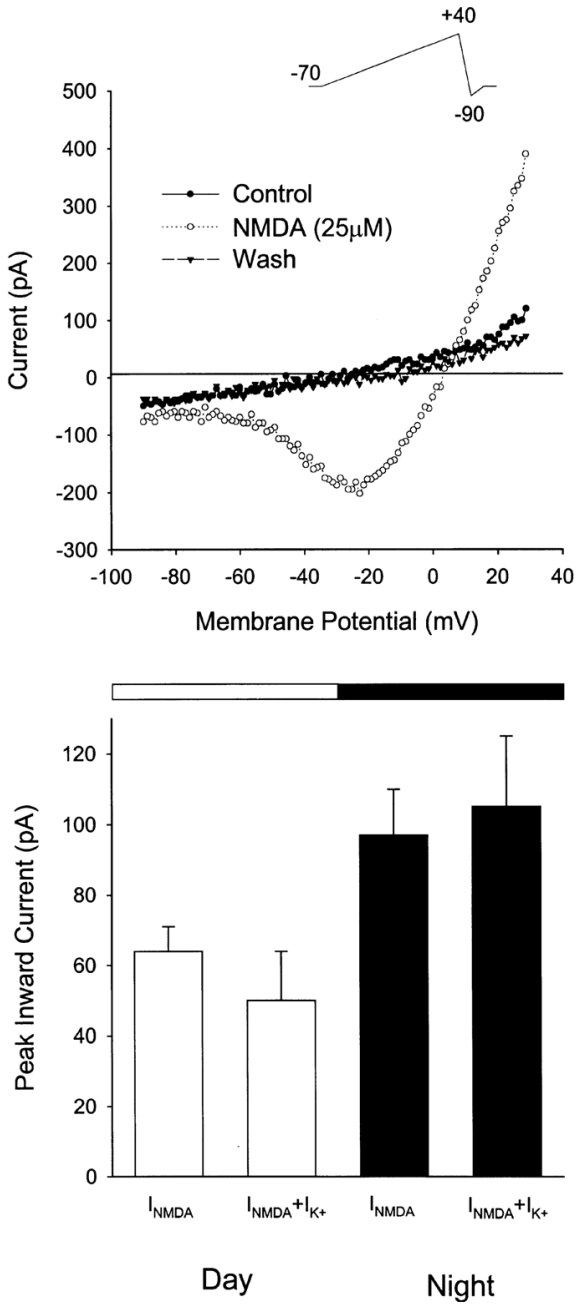

FIG. 5.

Daily rhythm in NMDA currents in SCN neurons. Whole-cell patch clamp recording techniques were used to directly measure currents evoked by NMDA in SCN neurons. The voltage-dependence of the NMDA-evoked currents was measured by moving the cell through a ramp of voltages (schematically illustrated in the top insert) before, during, and after treatment with NMDA in the bath. As with the imaging experiments, these responses were measured in the presence of TTX and methoxyverapamil. Top panel shows an NMDA response recorded using this protocol. All data were collected as the cell's membrane potential was moved from +40 mV to –90 mV. Bottom panel: NMDA currents were recorded in neurons in brain slices taken from animals during their day and compared to data obtained from brain slices from

animals during their night. These experiments were run in the absence of Mg^{2+} to reduce the voltage-dependence of the NMDA response and in the presence of cadmium (Cd^{2+}, 25 μM), and TTX (1 μM) in the bath. Under these conditions, there was a daily rhythm in NMDA-evoked inward currents ($I_{NMDA} + I_K$) with peak responses significantly ($P < 0.001$) higher during the night ($n = 14$) than during the day ($n = 11$). In other experiments, voltage-gated K^+ currents were also blocked with TEA in the bath and Cs^+ (125 mM) in the patch pipette. Under these conditions, there was also a daily rhythm in NMDA-evoked inward currents (I_{NMDA}) with peak responses significantly ($P < 0.05$) higher during the night ($n = 21$) than during the day ($n = 23$).